Hydrol. Earth Syst. Sci. Discuss., 2, 2521–2547, 2005
www.copernicus.org/EGU/hess/hessd/2/2521/
SRef-ID: 1812-2116/hessd/2005-2-2521
European Geosciences Union

Hydrology and Earth System Sciences Discussions

Papers published in *Hydrology and Earth System Sciences Discussions* are under open-access review for the journal *Hydrology and Earth System Sciences*

Vectors of subsurface stormflow in a layered hillslope during runoff initiation

M. Retter[1], **P. Kienzler**[2], **and P. F. Germann**[1]

[1]Department of Geography, University of Bern, Hallerstr. 12, 3012 Bern, Switzerland
[2]Institute of Hydromechanics and Water Resources Management, ETH Zürich, Schafmattstrasse 8, 8093 Zürich, Switzerland

Received: 7 November 2005 – Accepted: 12 November 2005 – Published: 30 November 2005

Correspondence to: M. Retter (retter@giub.unibe.ch)

Abstract

The focus is the experimental assessment of in-situ flow vectors in a hillslope soil. We selected a 100 m^2 trenched hillslope study site. During prescribed sprinkling an obliquely installed TDR wave-guide provides for the velocity of the wetting front in its direction. A triplet of wave-guides mounted along the sides of an hypothetical tetrahedron, with its peak pointing down, produces a three-dimensional vector of the wetting front. The method is based on the passing of wetting fronts. We analysed 34 vectors along the hillslope at distributed locations and at soil depths from 11 cm (representing top soil) to 40 cm (close to bedrock interface). The velocity vectors of the wetting fronts were generally gravity dominated and downslope orientated. Downslope direction (x-axis) dominated close to bedrock, whereas no preference between vertical and downslope direction was found in vectors close to the surface. The velocities along the contours (y-axis) varied widely. The Kruskal-Wallis tests indicated that the different upslope sprinkling areas had no influence on the orientation of the vectors. Vectors of volume flux density were also calculated for each triplet. The results of the vector approach are compared with hydrometric measurements such as subsurface stromflow, collected at the downhill end of the slope.

1. Introduction

For a wide range of hillslopes subsurface stormflow (SSF) is considered a major runoff generating process. For instance, Weyman et al. (1973) studied the direction and occurrence of the subsurface runoff component and found the following: Infiltration is driven by gravity and thus flow in slopes is dominated by vertical unsaturated movements towards the profile base, where lateral subsurface flow originates due to breaks in vertical permeability (distinct soil horizons or impermeable bedrock). They further argued that, once saturated conditions have been generated, lateral flow should occur, because the equipotential lines within the saturated soil will be nearly orthogonal to the

HESSD

2, 2521–2547, 2005

gradient of the slope. The authors mentioned also that runoff response will be considerably delayed if water has to move first to the base of the soil profile, but lateral flow controls the magnitude of hillslope response.

Harr (1977) used tensiometer plots to closer look into the magnitude and direction of water fluxes in a hillslope. Between storms the vertical flux component at the 10 cm-depth was inferior to the downslope (lateral) components, but similar during storms. Conversely, vertical flux components at the 70- and 130 cm-depths were inferior to the downslope components during storms but similar to downslope components between storms. Greminger (1984) calculated two-dimensional and Wheater et al. (1987) calculated three-dimensional soil water fluxes from tensiometer data. They monitored lateral components during dry conditions and after high intensity rainfall. They also determined the triggering factors such as slope angle, degree of saturation, hydraulic conductivity of soil horizons, and rainfall intensity. Anderson and Burt (1978) illustrated the influence of contour curvature (three-dimensional) on moisture movement.

Preferential flow in soil pipes occurs laterally above and within soil layers of lower permeability such as solid rocks and glacial tills or perched water tables (Sidle et al., 2000; Koyama and Okumura, 2002; Uchida et al., 2005). On the other hand, Beven and Germann (1982) considered infiltration, with its mainly preferential flow, as driven by gravity. Buttle and McDonald (2002) investigated preferential flow systems in a thin soil at a slope by an combined approach consisting of TDR wave-guides and water/solute studies. The former measurement indicated vertical infiltration whereas the latter focused on lateral flow towards a trench. Both, matrix flow and preferential flow have to bend from mainly vertical to the predominant lateral direction. However, the processes leading to the pattern are poorly understood. Sherlock et al. (2000) discussed the necessity to include the general uncertainty associated with hydrometric techniques in the subsurface (e.g. calculation of hillslope flow paths).

We present the results of an investigation on the direction of flow at the hillslope scale. We focus on the direction of the infiltration fronts that are associated with sprinkling and that lead to runoff.

HESSD

2, 2521–2547, 2005

The objectives of this paper are:

i.) How "vertical" is vertical infiltration?

ii.) Can we find evidence for "bending of flow" from the vertical to lateral?

iii.) How does the velocity vector of the wetting front relate to runoff concentration time?

iv.) What is the potential of the setup, to improve understanding of hillslope runoff?

2. Study site

The hillslope site was located at Lutertal, community of Reiden, northern Switzerland. We consciously selected a site where lateral SSF is likely to occur. Average annual precipitation at the site is 1056 mm. We marked off a $12 \times 16\,m^2$ plot, which has been under grassland during the past 30 years. The slope angle α was 13.5°. We excavated a trench at the bottom of the slope. The soil consisted of a top Ah-horizon (0–8 cm) and a sandy loam B-horizon with an average depth down to 45 cm. The particle size distribution in the B- horizon was 20% sand, 53.1% silt, and 22.9% clay by weight.

The underlaying bedrock is composed of siltstone (*Molasse*) with reduced hydraulic conductivity. Laboratory experiments showed the wetting front to propagate slowly with a mean velocity of $4 \times 10^{-6}\,mm\,min^{-1}$ (I. Willen-Hincapié, personal communication). At the trench face we observed vertical macropores, mostly created by earthworms (*Lumbricidae*), small lateral soil pipes (diameter 3–8 mm) occurred at the transition between the B-horizon and bedrock.

3. Methods

Germann and Zimmermann (2005) applied a novel approach to two runs at the 1-m^2-plot scale. This is now extended to the hillslope scale.

3.1. Basics on TDR application

One obliquely installed TDR wave-guide records the temporal increase of volumetric soil moisture θ [$m^3\,m^{-3}$] when the wetting front moves across them. This increase between the initial volumetric soil moisture θ_{ini} and the maximum volumetric soil moisture θ_{max} is outlined in Fig. 1. The direction of the vector component is set equal to the one of the wave-guide. The steady advancement of the wetting front during the interval t_U to t_L yields:

$$v_i = \frac{l_i}{t_{L,i} - t_{U,i}} = \frac{\Delta\theta_i}{\Delta t_i} \cdot \frac{l_i}{w_{max_i}} \quad (1)$$

where $w_{max} = \theta_{max} - \theta_{ini}$ [$m^3\,m^{-3}$], l is the length of wave-guides positioned between U_i (x,y,z) and L_i (x,y,z), t_U and t_L are the arrival times of the wetting front at U and L, and $\Delta\theta/\Delta t$ is the slope of $\theta(t)$ between t_U and t_L. Likewise, the vector of the average volume flux density, q [$m\,s^{-1}$], during $t_U<t<t_L$ in the direction of the wave guides is:

$$q_i = v_i \cdot w_{max_i} = l_i \cdot \frac{\Delta\theta_i}{\Delta t_i} \quad (2)$$

The index i ∈ (e, t, s) refers to the wave guides, Fig. 2. The procedure is repeated for the two other wave-guides. The resulting vectors $\boldsymbol{v}$ and $\boldsymbol{q}$ are built by the components V_e, V_t, and V_s respectively q_e, q_t, and q_s. Coordinate transformation results the vectors $\boldsymbol{v}$ and $\boldsymbol{q}$ in x, y, z space. Figure 2 shows the installation of one triplet, containing three TDR wave-guides, which are orthogonally aligned to each other. Figures 2 and 3 show the arrangement of the wave-guides in the coordinate system. The vector sum (norm vector) is:

$$v_{tot} = \sqrt{v_x^2 + v_y^2 + v_z^2} = |\boldsymbol{v}| \quad (3)$$

$$q_{tot} = \sqrt{q_x^2 + q_y^2 + q_z^2} = |\boldsymbol{q}| \quad (4)$$

The length of the TDR-wave guides is decisive on the sensitivity of the soil moisture measurements: The longer the wave-guides, the less sensitive the measurements will get. On the other hand, the longer the wave guides the larger the control volume of assessing the vectors. For field measurement wave-guides with a length between 0.15 m and 0.30 m are suggested as a compromise between the accuracy of travel time measurement, conductivity losses, and ease of installation (Robinson et al., 2003).

3.2. Instrumentation

3.2.1. TDR wave-guides

One TDR wave-guide consisted of two l=0.15 m long, parallel stainless steel rods, 30 mm apart and each 5 mm in diameter. The TDR wave-guides were electrically connected with a 50 Ω coax cable to a SDMX 50 coaxial multiplexer and further to a Campbell TDR 100 device, which generated the electrical pulses and received the signals. Both units were controlled by a Campbell CR 10x micro logger and the measurement interval was set to 90 s to more closely record the breakthrough of the wetting.

We distributed ten triplets of TDR wave-guides across the hillslope, Fig. 3. Wave-guide drill holes were sealed with bentonite. When pushing wave-guides into the soil we carefully paid attention to avoid gaps between steel rods and soil (Gregory et al., 1995) and to avoid changes in soil structure (Rothe et al., 1997). The depth varied between triplet spits close to soil surface (11 and 14 cm) to triplet spits at the boundary of soil-bedrock (27 and 35 cm). We located triplets in the way that sprinkled upslope contributing areas varied. Supplementary, a few oblique TDR wave-guides, called L1–L6, were installed 2–4 cm above the bedrock interface right into the trench face. We aligned those wave-guides within the plane formed by the h- and y-axis and situated them with an angle of 45° to the x-axis. Sheet metal canopies (20×35×0.4 cm) were pushed into the soil above L1–L6, but still parallel, with a clearance of 10 cm. Thus, they protected each of the six wave-guides against flow in z-direction. This setup allowed a direct measurement of the established lateral wetting front along the h-axis and on the

bedrock interface, where SSF is likely to occur.

To calculate volumetric water content, we used the transfer function by Roth et al. (1990), who separated the impacts on the dielectric number of the wave geometry from the soil properties such as bulk density and the content of clay in organic matter. For calibration prior to the installation in the field each wave-guide was totally submerged and the corresponding dielectric number was set equal to the volumetric water content of $1\,m^3\,m^{-3}$.

3.2.2. Sprinkling

The entire $100\,m^2$ hillslope segment was artificially sprinkled until SSF reached steady state. In order to account for different runoff concentration times we applied intensities of 11.5, 19, 35, and $56\,mm\,h^{-1}$, respectively. This range was achieved by different pumping pressures and two kind of systems: a sprinkler (design: Gardena) and a nozzle system by Rain Bird. Two automatic rainfall gauges, seven distributed rainfall samplers (manually checked every hour) and a water meter (sum normalized by measured sprinkling area) allowed to calculated the input precisely. Prior to experiments we optimized the homogeneity of sprinkling by several tests-runs. For details on the spatial distribution within the hillslope see Appendix A.

We also conducted sprinkling experiments on 1-m^2 plots. The rain simulator here consisted of 100 nylon tubes with inner diameters of 2 mm, which were mounted in a 0.1×0.1 m square pattern through a square of sheet metal of $1\,m \times 1\,m$. A gear moved the suspended sheet metal backwards and forwards ±50 mm in both horizontal dimensions such that it took approximately 1800 s for one tube outlet to return to the same spot. Distance between releases of drops down to the soil surface was 0.5 m. Controlled water supply was from a pump via a manifold to the tubes.

In addition, data of three natural storms were included in the analyses.

HESSD

2, 2521–2547, 2005

3.2.3. Tracer experiments

We carried out two kind of tracer experiments to track SSF. First, during sprinkling application of the entire slope Dirac delta spikes of Pyranin, Naphtionat and Uranin were fed into the sprinkler at early, mean, and late times. Flow in the hose towards the sprinkler was turbulent, ensuring that the tracer was well mixed by the time it reached the sprinkler or the nozzles. Tracers moved through the soil system and we took samples directly at the trench face to get tracer travel times.

Second, piezometer holes were used as two line sources of salt tracer (bromide, chloride) directly above the soil-bedrock interface at 4 and 8 m upslope from of the trench (see Fig. 3). The tracer was quickly injected. Sampling at the trench face allowed calculating tracer front velocity, which was determined by distance divided by time of first arrival minus the time of injection. Thus, it is a direct measure of presumed lateral flow along the bedrock.

Generally, the time interval of sampling was 60 s at the trench face and for total SSF, until flow stopped. We averaged the calculated tracer front velocities from different soil pipes in order to get mean travel times through the hillslope system.

3.2.4. Piezometers and monitoring of flow

The site had twelve piezometers, which reached to the bedrock at the bottom end. The inner diameter of the tube was 3 cm. At five piezometers a pressure transducer allowed automatic readings of water levels, and eight served as the tracer source (Fig. 3). Additionally, flow collectors and tipping buckets to capture SSF were installed at the trench. We also monitored overland flow by flow collectors and tipping buckets.

4. Results

A total of 123 wetting fronts were recorded by TDR wave-guides. They were generated either by 1-m^2 plot irrigation, entire sprinkling of the hillslope or natural rain events. Fig-

ure 4 shows a breakthrough of wetting at the TDR wave-guides of one triplet. For all data the increase in soil moisture averaged to 6.2%vol. The coefficients of determination, R^2, of the linear regressions of θ(t) between t_U and t_L exceeded 0.9 for 66 wetting fronts. We ignored 21 wetting fronts, as they were not a complete set of the three components. Thus, from the total number of velocities at the TDR wave-guides, 34 datasets on triplets (equal to 102 single velocities) were finally derived. To enhance readability velocities are set in mm min^{-1}. Table 1 lists the components and resultants of the vectors that are described by the means v_x=12.5 mm min^{-1}, v_y=for −1.1 mm min^{-1} and v_z=5.7 mm min^{-1}.

The vectors within the soil are six orders of magnitude faster than in the under laying bedrock. This shift of velocities caused repressed water at the soil bedrock interface. Water generated lateral flowpaths on the sloping bedrock interface within the hillslope.

An overview of all vectors is given by 2-D hillslope slices (Fig. 5). The results are plotted in a log-log scale, as dimensions differ over two orders of magnitude. However, Figs. 5b and c presume that no value with y=0 occurred (as they are not defined by the logarithm). No value of y<0.1 occurred and negative log numbers simply indicate a different orientation rather than true negative numbers.

Vectors of the triplets A, B, and C from repeated 1-m^2 sprinkling events on equal intensities were analyzed by paired samples t-tests. Since the significant value for all three cases is around 0.29, we conclude that the results are reproducible for same sprinkling intensities and thus no change in xz-direction occurred.

Correlations between the different depths of the triplets and vector sum v_{tot} were not detectable (R^2=0.42, n=33). No significant relation was found between sprinkling intensity and v_{tot} for all data (R^2=0.25, n=33) and neither one for sprinkling intensity and spatial orientation of the velocity vector.

Initial soil moisture conditions varied over 11%vol for all data and 5%vol for all data generated by hillslope sprinkling experiments. The higher θ_{ini}, the less data are available up to "wet" conditions for a precise determination of slope of θ(t) between t_U and t_L. Thus, we got best fitting results for the slope between $t_U$and t_L when the initial hill-

HESSD
2, 2521–2547, 2005

slope system was driest (ID # 12–16). We tested correlations of θ_{ini} conditions with v_{tot} and also with the amount of increasing soil moisture during infiltration. For both cases no significant correlations were found.

The time series of θ after sprinkling showed an extended tailing of up to 4 days until initial soil moisture conditions were reached again. This pattern was more dominant for deep triplets and for data concerning the experiments in November (ID # 1–11), when transpiration was negligible. The long-tailed pattern is shown in Fig. 4.

4.1. Analysis of x- y- z- velocity components during infiltration towards spatial dominant direction

Of main interest is the view in the y-direction of contours i.e., looking at the x-z plane in our notation, Fig. 5a. The ID numbers and corresponding alphabetic code refer to the location of triplets on the hillslope. All vectors show a downhill component. The dominance of the z- against the x-components was checked with a t-test for all data (see Table 2). A significance value of the test of 0.1 was selected because pattern should trace clearly. Presuming this significance value, we could not find z- or x-components dominating except for the vectors at depth ≤ -28 cm and ≤ -35 cm where the x-components excelled the z-components (see bold numbers). But still, the mean angle of the fronts is 11° and 18° steeper than the h-axis. Thus, we do not consider it fully lateral.

The observed direction in the xy-plane (Fig. 5b) is widely aligned around y=0. By means of the t-test, a dominating x-direction (a downhill force rather than a spreading along the contours) is proposed. This is even confirmed by a strong significance value of 0.05. The fast velocities (ID # 11, 15, 16) concerned the shallow triplets K and E, where TDR rods are easily approachable after 5–10 cm of Ah-horizon.

The yz-view (Fig. 5c) reveals the dominance z-direction, which is supported by a significant value <0.05 (t-test). The above mentioned fast velocities at the shallow triplets also trace in this view. To conclude the wide spreading distribution along the y-axis (coefficient of variation: −8.4), there is heterogeneity in the soil, but the mean of velocities levelled to $-1.1\,\mathrm{mm\,min^{-1}}$.

As triplets B, C, F, and J are located at the same depth, we also addressed the question of the effects of differing upslope sprinkling area on orientation. Using data of 11 mm h^{-1} sprinkling, we analysed the resulting vector of the infiltration front for xz-components. The Kruskal-Wallis test (Kruskal and Wallis, 1952) told that the ratings of the resulting vector (its orientation towards a lateral component) did not differ by the upslope sprinkling area (chi-square= 3, asymp. sig.=0.392).

The question of scale: do vector components for same triplets differ between 1-m^2 sprinkling and hillslope sprinkling? This could merely be investigated for given intensities of 55 mm h^{-1} and given equal antecedent soil moisture for triplets A and C, where we emphasised on the xz-components. Here, we refrained to apply a test, as numbers were too small. But from a visual check of Fig. 5 the direction of the wetting front changed moderately between the two types of sprinkling.

The lateral vectors of SSF at the trench face were analysed on the basis of the mean average of L1 to L5. For the 1-m^2 plot sprinkling events ID # 21, 22 it amounted to 2.5 mm min^{-1}. And for the entire hillslope event on 14 June 2005 the front velocity was calculated to 4.6 mm min^{-1}.

4.2. Time to concentration of runoff and tracer travel times

SSF, initiated by sprinkling, flowed into the trench through up to nine soil pipes. Except two (where L2 and L3 were installed) all flow pathways where not visible until the first runoff indicated an active pipe. These horizontal preferential pathways contributed almost the total SSF, and very little percolation out of the matrix occurred. Pipe outlets were located close to the soil-bedrock interface showing the existence of microchannels according to Sidle et al. (2001). The same soil pipes were repeatedly active. The characteristics of the SSF as time to concentration and mean tracer velocity are shown in Table 3. Time to concentration of SSF, calculated as lag time between start of sprinkling to start of SSF, varied between 43 and 120 min. It depended on sprinkling intensity (R^2=0.98). That means, we always had the same initial loss in mm.

During sprinkling five Dirac delta pulses of tracer allowed to measure travel times

by the first tracer arrival at the trench face. For saturated conditions, as indicated by the piezometers, it varied between 7 and 13 min depending highly on the sprinkling intensity (Table 3). Thus, tracer travel times during wet conditions and active runoff at the trench were 5 to 10 times faster than initial time to concentration of flow. During almost initial conditions on 14 June 2005 when one tracer was fed into sprinkling 20 min past start of sprinkling, the tracer travel time resulted 80 min, which was similar than time to concentration (74 min).

Line source tracer experiments in 8 m distance to the trench were carried out, when piezometers indicated saturated conditions (10–15 cm) above the bedrock interface. The tracer front velocity resulted 658 mm min^{-1}. For the same conditions tracer front velocity regarding the 4 m tracer line amounted to 375 mm min^{-1}.

We also calculated volume flux densities according to Eq. (2) which also resulted in a three-dimensional vector. This was needed to get the vector sum q_{tot}, which ranged between 0.9 and 61.6 mm min^{-1} (Table 1). The mean amount was 13.4 mm min^{-1}.

4.3. Water balance calculations

Water balance calculations for the entire experiment on 3 November 2004 with 11 mm h^{-1} of sprinkling intensity showed: Input 151 mm, overland flow: 2.2 mm, SSF: 54 mm, soil storage: 33.2 mm, and losses 62 mm. To produce SSF 30 mm were needed.

For the experiment on 12 November 2004, with a sprinkling intensity of 19 mm h^{-1}, water balance calculations are the following: Input 97.5 mm, overland flow: 3.5 mm, SSF: 28 mm, soil storage: 43.5 mm, and losses 22.5 mm. Here, SSF occurred after 32 mm of sprinkling.

HESSD
2, 2521–2547, 2005

5. Discussion

The vectors are reproducible among repeated experiments, which is in accord with Germann and Zimmermann (2005). The direction of the vectors also matches well with the direction of that previous study and both data plot within the same order of scale, although soils are different. The bending of vectors, due to backlogging of water from the run just before, which Germann and Zimmermann (2005) showed, could not be observed in these data, as repeatable runs here were far off each other.

5.1. Discussion of temporal patterns

Here, we emphasis on the discussion of temporal hillslope response and concentration times and the link to velocities calculated by the triplets. Looking at the lateral velocity of the wetting front (determined as h-component at waves-guides L1–L6 and at triplets close to bedrock interface) and the travel times obtained by tracer data during steady state conditions we conclude: The lateral velocities (along h-axis) of first line source tracer arrival onto the bedrock are 140 and 80 times higher than for the vector of wetting front. The difference is obvious as conditions shift from unsaturated to saturated for this shallow layer onto the bedrock while discharge at the trench face occurred. Our observations of temporal patterns in the unsaturated zone are different from rapid pore pressure responses and the direct control of timing and magnitude of peak discharge (Torres et al., 1998).

5.2. Uncertainties and limitations involved in the approach

A major concern on the application of this approach at the Lutertal field site is the dominating runoff generation mechanism. The lateral SSF is delivered by preferential flow in soil pipes occurring at the trench face. For the z-direction there is evidence of macropores within the sandy loam B-horizon beside matrix infiltration. Thus, we deal with preferential pathways rather than with a homogenous matrix. It is likely that

HESSD

2, 2521–2547, 2005

water bypassed the wave-guides with their lengths / of 15 cm. Up to now, the length of the TDR wave guide has not been changed. We will work on that task in upcoming investigations in order to sufficiently trace preferential flowpaths.

The results presented state the moment of initial infiltration of the wetting front. They provide evidence for "bending of flow" from a vertical to a lateral component, which was seen in Table 2, last row. But an obvious lateral vector, aligned on the h-axis is not supported with the data. We may further question: a.) Why was there no significant change of h-components as the upslope contributing area (catchment area) increased and b.) why was there a minor dominance in x- or h-direction for deep triplets, although SSF occurred? To answer these questions we must highlight the fact that lateral flow is delayed with respect to infiltration. After the infiltration front passed steady state occured. At this point of time there is very limited increase of volumetric soil moisture possible because of limited total porosity. The TDR technique in general does not allow to extract any further information on the volume of flux passing by. Showing a major restriction of the vector method.

In order to compare average volume flux density q by the TDR wave-guides with discharge data of the trench, we assessed the representative elementary cross-sectional area (RECA). A discussion on that was introduced by Germann and Zimmermann (2005) who determined the bottom area of the truncated tetrahedron to 0.02 m^2. The sampling volume of TDR wave-guides is widely modelled by numerical approaches (Ferré et al., 1998, 2001) which may help to get a cross sectional area corresponding to the volume flux density of the triplet. In a first assumption the projection of the TDR rods might be used. Comparisons between q at the triplets and a calculated flux density at the trench face ($16 \times 0.45\ m^2$) for steady state SSF do stress time scales of both measures.

5.3. Further steps

Concluding the last sections we see a need to verify the approach presented here and quantitatively link it to discharge data. One useful option to elucidate this is a flow

transport model. This would allow comparing the velocity information at triplets and the SSF gauging with the modeled numbers of both measures. On the other hand, the data provided in this work emphasizes on the wetting front. For this consideration kinematic wave approximations for subsurface flow in hillslopes reveal as simple but efficient solutions. Here, we see an useful link to the work of Cabral et al. (1992) who showed in their Fig. 2 the dimensional analysis of unsaturated flow and its x, z, and volume flux-vectors.

Further, to gain understanding of postponed lateral flow and recorded bending of flow, we must extend the approach and integrate data of the decreasing limb of soil moisture. For the performed steady state experiments the shape of recession branch did not allow to extract more information because of the long tailing of θ.

6. Conclusions

We could find the following answers to our questions:

i.) Vertical infiltration and its propagating fronts do not move truly vertically, as we have shown in this exercise. None of the vectors was an exclusive z-component. Soil heterogeneity causes deviation up to an angle of 67° from the z-axis.

ii.) The presented approach allowed us to determine the spatial direction of the advancing wetting front. This is restricted to the first passing through of wetting! Thus, up to now the approach is insufficient to fully demonstrate the "bending of flow" while lateral components are mostly delayed to infiltration. However, several deep triplets provide evidence for lateral components as discussed above.

iii.) For the Lutertal field site we gained knowledge that lateral saturated tracer movement on top of the bedrock are 25–140 times faster than lateral unsaturated zone velocities of the wetting front. The vector velocities ranged in the scale of 0.1 to 89 mm min^{-1}. Time to concentration was sprinkling rate dependent and ranged

HESSD
2, 2521–2547, 2005

between 43 and 120 min for the site. No significant relation was found between concentration time and lateral velocity or the vector sum v_{tot}.

iv.) This method is restricted to non-complex substrate (skeleton or portion of big stones) to install TDR wave-guides. A plane bedrock topography with its similarity to the simple surface topography is of further help. This method is restricted to the first wetting front arriving while sprinkling or a rain storm occurs. The uncertainty of this method, e.g. dominance of preferential pathways during runoff, questions the transferability of l=15 cm wave-guide information towards a hillslope of 100 m^2. Quantitative comparisons between measured outflow at the trench and volume flux at the triplet are not possible up to date. We believe that there is useful information included, but there is a need to extend the approach.

Acknowledgements. We highly appreciated the input of I. Willen-Hincapié. F. Schärer guaranteed access to the research site and helped with useful farming support. This project was funded by the Swiss National Research Foundation (#200020-101562).

References

Anderson, M. G. and Burt, T. P.: The role of topography in controlling throughflow generation, Earth Surface Processes and Landforms, 3, 331–344, 1978.

Beven, K. and Germann, P.: Macropores and waterflow in soils, Water Resour. Res., 18, 1311–1325, 1982.

Buttle, J. M. and McDonald, D. J.: Coupled vertical and lateral preferential flow on a forested slope, Water Resour . Res., 38, WR000773, 2002.

Cabral, M. C., Garrote, L., Bras, R. L., and Entekhabi, D.: A kinematic model of infiltration and runoff generation in layered and sloped soils, Adv. Wat. Res., 15, 311–324. 1992.

Ferré, P. A., Knight, J. H., Rudolph, D. L., and Kachanoski., R. G.: The sample areas of conventional and alternative time domain reflectometry probes, Water Resour. Res., 34, WR02093, 1998.

Ferré, P. A., Nissen, H. H., Moldrup, P., and Knight, J. H.: The sample area of time domain reflectometry probes in proximity to sharp dielectric permittivity boundaries, p. 195–209, in:

2nd Proc. Int. Symp. and Workshop on Time Domain Reflectometry for Innovative Geotechnical Applications, available at: http://www.iti.northwestern.edu/tdr/tdr2001/proceedings/Final/TDR2001.pdf (verified 15 July 2005), edited by: Dowding, C. H., Infrastructure Technology Institute, Northwestern University, Evanston, IL, 2001.

Germann, P. F. and Zimmermann, M.: Directions of preferential flow in a hillslope soil. Quasi-steady flow, Hydrological Processes, 19, 887–899, 2005.

Gregory, P. J., Roland, P., Eastham, J., and Micin, S.: Use of time domain reflectometry (TDR) to measure the water content of sandy soils, Aust. J. Soil Res., 33, 265–276, 1995.

Greminger, P.: Physikalisch-ökologische Standortsuntersuchung über den Wasserhaushalt im offenen Sickersystem Boden unter Vegetation am Hang, Eidg. Anstalt forstl. Versuchswes., Mitt. 60, 151–301, 1984.

Harr, R. D.: Water flux in soil and subsoil on a steep forested slope, J. Hydrol., 33, 37–58, 1977.

Koyama, K. and Okumura, T.: Process of pipeflow runoff with twice increase in discharge for a rainstorm, Trans. Jpn. Geomorphol. Union, 23, 561–584, 2002.

Kruskal, W. H. and Wallis, W. A.: Use of ranks in one-criterion variance analysis, J. Amer. Stat. Assoc., 47(260), 583–621, 1952.

Robinson, D. A., Jones, S. B., Wraith, J. M., Or, D., and Friedman, S. P.: A Review of Advances in Dielectric and Electrical Conductivity Measurement in Soils Using Time Domain Reflectometry, Vadose Zone J., 2, 444–475, 2003.

Roth, K., Schulin, R., Flühler, H., and Attinger, W.: Calibration of time domain reflectometry for water content measurements using a composite dielectric approach, Water Resour. Res., 26, WR01238, 1990.

Rothe, A., Weis, W., Kreutzer, K., Matthies, D., Hess, U., and Ansorge, B.: Changes in soil structure caused by the installation of time domain reflectometry probes and their influence on the measurement of soil moisture, Water Resour. Res., 22, WR0474, 1997.

Sherlock, M. D., Chappell, N. A., and McDonnell, J. J.: Effects of experimental uncertainty on the calculation of hillslope flow paths, Hydrological Processes, 14, 2457–2471, 2000.

Sidle, R. C., Noguchi, S., Tsuboyama, Y., and Laursen, K.: A conceptual model of preferential flow systems in forested hillslopes: evidence of self-organization, Hydrological Processes, 15, 1675–692, 2001.

Sidle, R. C., Tsuboyama, Y., Noguchi, S., Hosoda, I., Fujieda, M., and Shimizu, T.: Storm flow generation in a steep forested headwater: a linked hydrogeomorphic paradigm, Hydrological

Processes, 14, 369–384, 2000.
Torres, R., Dietrich, W. E., Montgomery, D. R., Anderson, S. P., and Loague, K.: Unsaturated zone processes and the hydrologic response of a steep unchanneled catchment, Water Resour. Res., 23, WR01140, 1998.
Uchida, T., Tromp-van Meerveld, I., and McDonnell, J. J.: The role of lateral pipe flow in hillslope runoff response: an intercomparison of non-linear hillslope response, J. Hydrol., 311, 117–133, 2005.
Weyman, D. R.: Measurements of the downslope flow of water in a soil, J. Hydrol., 20, 267–288, 1973.
Wheater, H. D., Langan, S. J., Miller, J. D., and Ferrier, R. C.: The determination of hydrological flow paths and associated hydrochemistry in forested catchments in central Scotland, IAHS Pub. No. 167, Proc. Vancouver Symposium, 1987.

Table 1. Components of velocities and volume flux densities in spatial xyz-space for triplets during different sprinkling events.

ID #	Date	Type of sprinkling	Velocity of wetting front [mm min^{-1}]			Volume flux density [mm min^{-1}]				Triplet	Depth of TDR tip [cm]
			V_x	V_y	V_z	q_x	q_y	q_z	q_{tot}		
1	3 Nov. 2004	hillslope	1.5	−0.2	0.4	0.8	−0.1	0.2	0.9	A	35
2	3 Nov. 2004	hillslope	6.8	0.3	1.8	3.8	0.1	1.0	3.9	B	28
3	3 Nov. 2004	hillslope	2.9	−0.6	1.2	1.7	−0.3	0.7	1.9	C	28
4	3 Nov. 2004	hillslope	3.3	−0.2	1.5	1.9	−0.1	0.8	2.1	D	40
5	3 Nov. 2004	hillslope	8.9	4.2	1.7	2.0	−0.5	1.6	–	E	11
6	3 Nov. 2004	hillslope	3.4	−0.8	2.5	5.8	−1.3	2.8	2.6	F	28
7	3 Nov. 2004	hillslope	10.1	−2.1	5.2	1.2	−0.3	0.2	6.5	K	15
8	3 Nov. 2004	hillslope	1.0	0	0.5	6.7	1.1	0.5	–	J	28
9	12 Nov. 2004	hillslope	2.1	−0.5	0.5	14.3	−7.8	24.9	1.2	A	35
10	12 Nov. 2004	hillslope	12.0	2.0	1.0	17.3	−1.6	14.8	6.8	B	28
11	12 Nov. 2004	hillslope	24.0	−13.4	42.9	18.4	1.8	3.0	29.8	E	11
12	27 May 2005	hillslope	31.0	−2.9	26.5	11.6	−1.8	9.1	22.8	A	35
13	27 May 2005	hillslope	32.6	3.2	5.6	24.0	−15.9	54.4	18.8	B	28
14	27 May 2005	hillslope	20.1	−3.1	15.2	50.1	21.7	23.2	14.8	C	28
15	27 May 2005	hillslope	38.4	−25.6	86.8	3.4	−0.9	1.5	61.6	E	11
16	27 May 2005	hillslope	89.2	34.8	38.6	4.4	0.4	2.6	59.3	K	15
17	20 May 2005	1 m^2	6.2	−1.6	2.8	3.8	0.5	0.8	3.8	A	35
18	13 May 2005	1 m^2	8.1	0.8	4.7	5.2	−1.6	1.4	5.1	A	35
19	13 May 2005	1 m^2	6.7	0.9	1.5	2.4	−1.3	2.8	3.9	B	28
20	20 May 2005	1 m^2	8.8	−2.9	2.4	11.5	0.1	12.8	5.6	C	28
21	7 June 2005	1 m^2	4.4	−2.3	5.2	3.7	−0.3	2.1	3.9	A	35
22	7 June 2005	1 m^2	20.8	0.2	21.8	12.3	−1.6	3.4	17.2	C	28
23	16 July 2005	1 m^2	7.0	−0.5	4.0	6.6	0.4	2.7	4.3	A	35
24	16 July 2005	1 m^2	22.2	−3.1	6.8	21.6	4.2	13.5	12.8	B	38
25	16 July 2005	1 m^2	11.8	0.8	5.3	0.8	−0.1	0.2	7.1	C	28
26	16 July 2005	1 m^2	35.9	7.1	23.6	3.8	0.1	1.0	25.8	E	11
27–34	26 Oct. 2004	Natural rain event on hillslope	*	*	*	*	*	*	*	A–E	*

HESSD

2, 2521–2547, 2005

Table 2. Values of t-test to analyse x- and z-components for the dominating direction of the resulting vector.

Selected triplets	Total number of vectors	t-test		
		Test value, T	Degrees of freedom, df	Sig. (2-tailed)
All (Natural events, sprinkling of hillslope, and 1 m^2 plots)	34	1.184	66	0.241
Sprinkling of hillslope	15	0.046	28	0.964
Sprinkling of all 1 m^2 plots	10	1.324	18	0.202
Sprinkling of deep 1 m^2 plots A, B, C	9	1.551	16	0.140
All data of shallow triplets E, K	8	0.116	14	0.909
All data of deep triplets A, B, C, D, F; where z≥28 cm	25	1.870	48	**0.068**
Sprinkling of deepest triplets A, D; where z≥35 cm	8	2.66	14	**0.019**

Table 3. Characteristics on the generation of subsurface stormflow (SSF) and results of tracer applications.

	3 Nov. 2004	12 Nov. 2004	27 May 2005	14 June 2005	14 June 2005	14 June 2005
Sprinkling intensity [mm/h]	11.5	19	56	32	32	32
Time to concentration of SSF (lag time from start of sprinkling to start runoff) [min]	120	104	43	74	74	74
Tracer application by sprinkling						
Time of tracer input, Dirac spike [min since start of sprinkling]	238	–	109	50	105	152
Time of first arrival [min since start of sprinkling]	251	–	116	130	137	158
Time of max. concentration [min since start of sprinkling]	257	–	128	135	–	–
Travel time of tracer, input until first arrival [min]	13	–	7	80	25	8
Degree of saturation for lower hillslope segment	full	–	full	little	less	full
(point measurements at 40 cm depth, piezometers) at moment of tracer application						
Tracer line source at piezometers						
Time of tracer input [min since start of sprinkling]	240	–	110	–	–	–

HESSD
2, 2521–2547, 2005

Appendix A

Table A1. Sprinkling intensity measured by seven randomly, spatially distributed point measurements on the hillslope. Mean and standard deviation of the data are provided in the down right corner. Data concern the experiment on 3 November 2004.

Sampler	Sprinkling intensity [mm h^{-1}] for 1 h of sprinkling while entire experiment											
1	10	5	3	13	10	13	15	17	18	11	12	8
2	11	9	9	13	10	13	13	10	11	13	9	8
3	11	10	14	12	9	12	9	8	9	0	7	9
4	14	16	18	18	15	24	24	23	35	24	17	12
5	10	11	10	13	10	10	10	10	12	11	9	4
6	10	8	11	13	9	10	9	9	12	9	5	9
7	10	8	10	10	8	8	10	9	11	11	8	13
										mean		11.5
										stddev		4.6

HESSD

2, 2521–2547, 2005

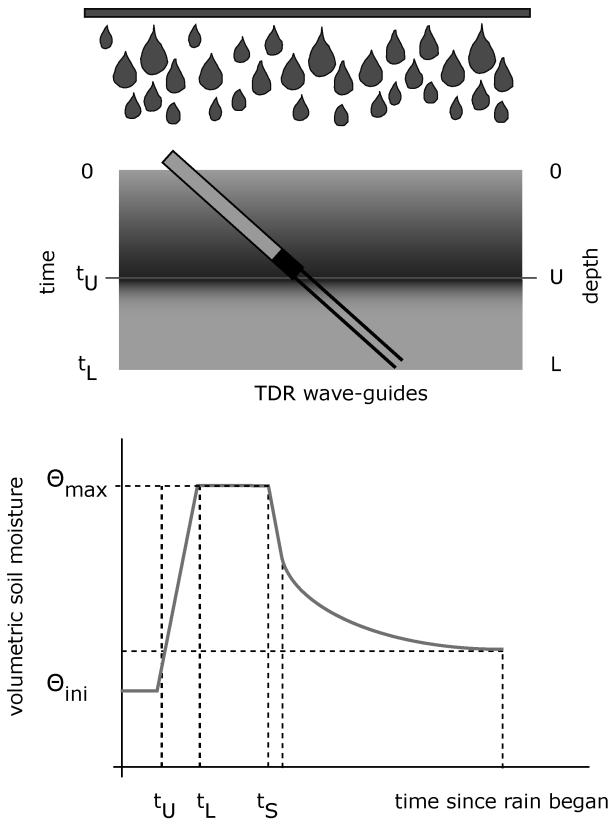

Fig. 1. Schematic representation of oblique installed wave-guide and a downwards travelling wetting front (up) and the linear increase of θ as the wetting front moves steadily (below). t_S indicates end of sprinkling.

HESSD
2, 2521–2547, 2005

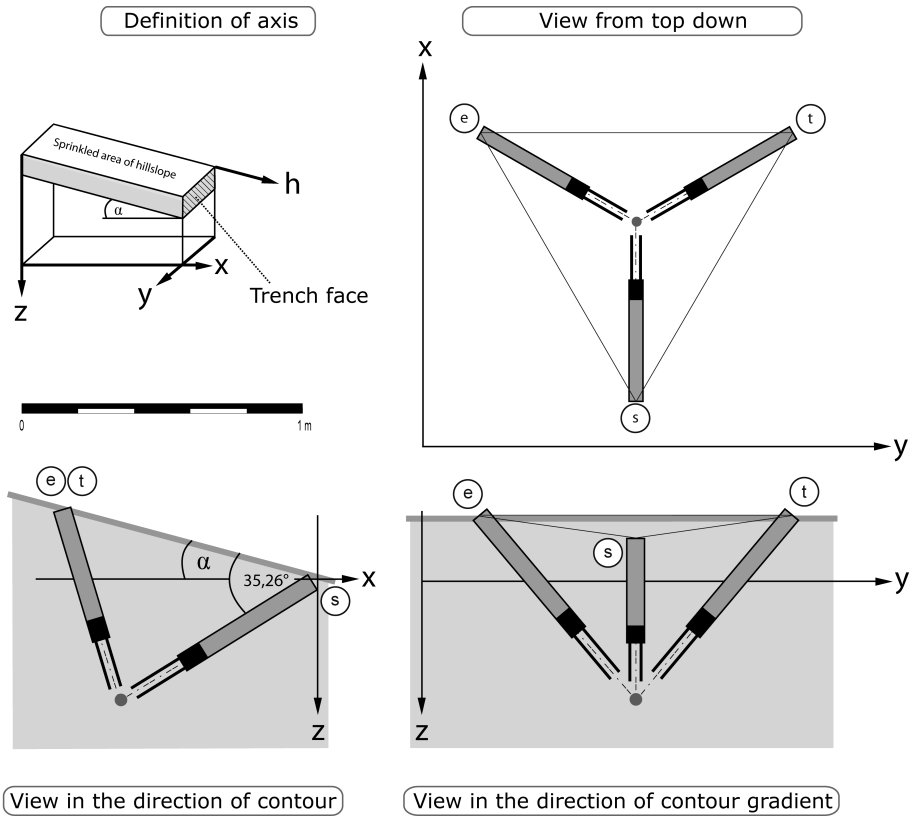

Fig. 2. Definition of axis (top left) and scheme of mounting a triplet of TDR wave-guides in a hillslope soil by its different views. Note that y-axis becomes positive towards right and negative towards left. And z-axis becomes more positive with increasing depth.

HESSD
2, 2521–2547, 2005

Vectors of subsurface stormflow in a layered hillslope

M. Retter et al.

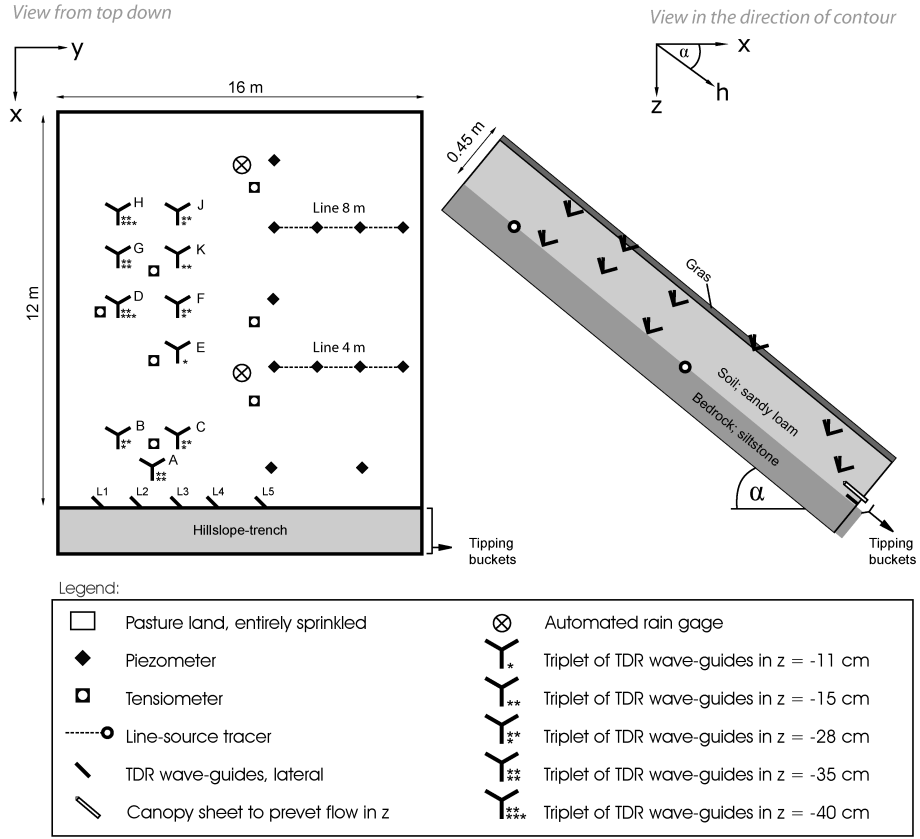

Fig. 3. Instrumentation and setup of TDR triplets at hillslope. Left: top down view; right: view in the direction of contour (profile).

HESSD
2, 2521–2547, 2005

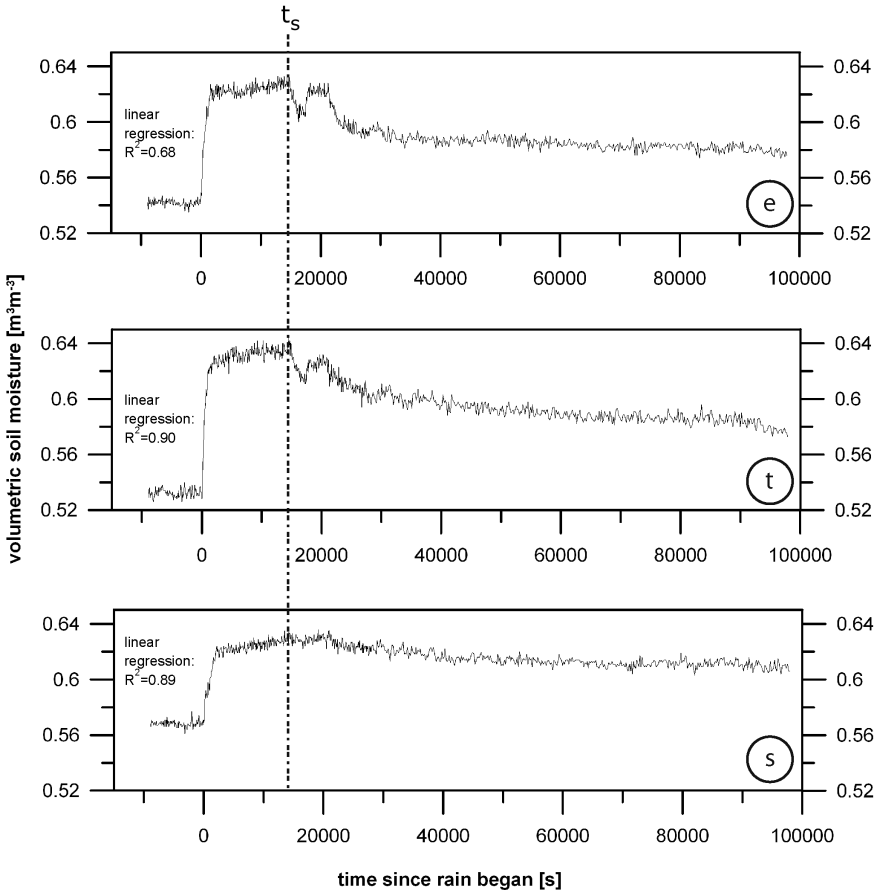

Fig. 4. Time-series of volumetric soil moisture for the three TDR wave-guides e, t, and s of triplet, ID 15. A linear regression between t_U and t_L is assumed and coefficients of determination are mentioned for each break-through of wetting on the left side.

HESSD
2, 2521–2547, 2005

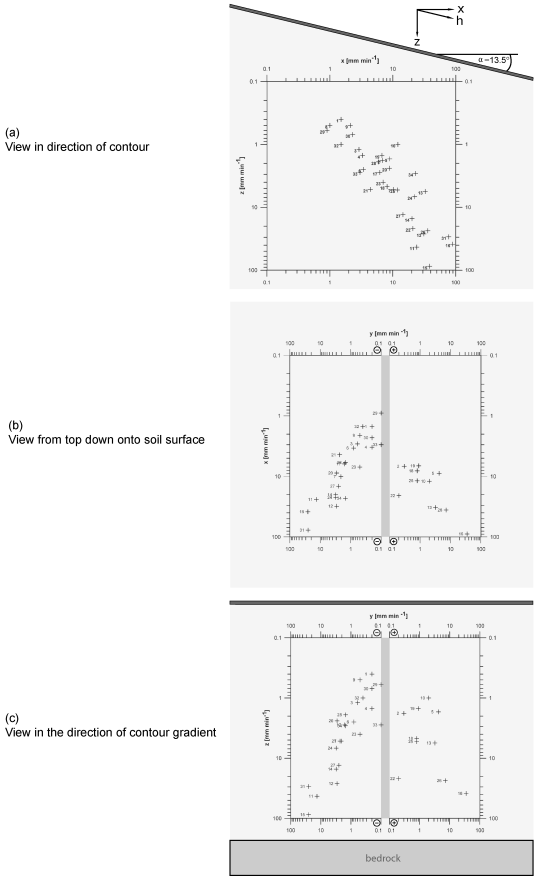

Fig. 5. Resulting velocity vectors of the wetting front at various triplets of the hillslope. Vectors are not shown in arrow format, due to readability, but start at the origin of coordinate systems. Given ID numbers refer to information provided in Table 1. Supporting orientation on the different views and coordinate systems was given in Fig. 2.

HESSD
2, 2521–2547, 2005